OPTICS

Breathing dissipative solitons in mode-locked fiber lasers

Junsong Peng[1], Sonia Boscolo[2], Zihan Zhao[1], Heping Zeng[1]*

Dissipative solitons are self-localized coherent structures arising from the balance between energy supply and dissipation. Besides stationary dissipative solitons, there are dynamical ones exhibiting oscillatory behavior, known as breathing dissipative solitons. Substantial interest in breathing dissipative solitons is driven by both their fundamental importance in nonlinear science and their practical applications, such as in spectroscopy. Yet, the observation of breathers has been mainly restricted to microresonator platforms. Here, we generate breathers in a mode-locked fiber laser. They exist in the laser cavity under the pump threshold of stationary mode locking. Using fast detection, we are able to observe the temporal and spectral evolutions of the breathers in real time. Breathing soliton molecules are also observed. Breathers introduce a new regime of mode locking into ultrafast lasers. Our findings may contribute to the design of advanced laser sources and open up new possibilities of generating breathers in various dissipative systems.

INTRODUCTION

The notion of dissipative solitons (DSs) in a nonlinear medium arises from the composite balance between conservative effects (nonlinearity and dispersion/diffraction) and dissipative ones (gain and loss) (*1*). DSs are universal in nature and are found in various subfields of natural science, including nonlinear optics, hydrodynamics, plasma physics, field theory, solid-state physics, chemistry, molecular biology, and many others (*2*). In addition to parameter-invariant stationary DSs, many nonlinear systems support breathing (pulsating) DSs, the energy of which is localized in space but oscillates in time, or vice versa. Breathers were first observed experimentally in passive optical fiber cavities (*3*) and subsequently reported in optical microresonators (*4*, *5*). These nonlinear waves are attracting considerable research interest in optics owing to their strong connection with the Fermi-Pasta-Ulam paradox (*6*, *7*), formation of rogue waves (*8*, *9*), turbulence (*10*), and modulation instability (*11*) phenomena. Apart from their fundamental importance in nonlinear science, breathing solitons are also attractive because of their potential for practical applications. For example, it has been recently demonstrated that breathers can increase the resolution of microresonator-based dual-comb sources (*12*).

In addition to their widespread use as sources of ultrashort pulses for many applications, mode-locked lasers constitute an ideal platform for the fundamental exploration of complex dissipative nonlinear dynamics. Various notable nonlinear phenomena have been observed in mode-locked lasers, including rogue waves (*13*, *14*), soliton molecules and molecular complexes *(15–18)*, pulsations of soliton bunches (*19*), and soliton explosions (*20–22*). Furthermore, a recent theoretical work using the master equation approach (*23*) has showed that there are regimes of operation in which laser oscillators may generate breathing solitons with large ratios of maximal to minimal energies in each period of pulsation. The soliton spectra also experience large periodic variations. However, to date, the experimental observation and characterization of these lasing regimes is challenging because of the fast evolutionary behavior of breathers, beyond the speed of traditional measurement tools. Notwithstanding, it is of great interest to investigate the excitation of breathing solitons in mode-locked lasers. Breather lasers can potentially be used as direct sources of supercontinuum light (*23*), and the periodic variation in output pulse parameters provided by these lasers can be exploited in applications (*12*). Moreover, from a practical viewpoint, stable ultrashort pulses are often considered of interest. However, dissipative systems admit stable pulses in a certain range of parameters, beyond which pulses may change periodically or chaotically on propagation. Therefore, accurate knowledge of the conditions for the occurrence of breathers is required to design systems to avoid them. Capturing the evolutionary behavior of breathing solitons requires real-time spectral and temporal measurements. Mode-locked lasers afford effective resolution of the spectral evolution of fast processes by means of the time-stretch dispersive Fourier transform (TS-DFT) technique (*24–26*), whereas the high repetition rates (>10 GHz) of breathers in microresonators hinder real-time TS-DFT spectral measurements.

Here, we report on the direct experimental observation of breathing DSs in a passively mode-locked fiber laser. Breathers are excited in the laser under the pump threshold for stationary mode locking. Breathing solitons feature periodic spectral and temporal evolutions over cavity round trips. We capture such fast dynamics spectrally and temporally in real time using TS-DFT–based single-shot spectral measurements (*24*) and spatiotemporal intensity measurements. These breathers are intrinsically different from those observed in microresonators because they are generated in the normal dispersion regime of the laser cavity; hence, they have distinguished rectangular spectra. Breathing soliton pair molecules are also generated in the cavity, which represent double-breather bound states with a close intrapulse separation. Breather molecules were recently demonstrated in a conservative optical fiber system (*27*). Numerical simulations of the laser model described by the complex Ginzburg-Landau equation support our experimental findings. Recently, Du *et al.* (*28*) reported on the experimental observation of different kinds of pulsating DSs in a mode-locked fiber laser. In that work, adjustment of the laser state from stationary to pulsating was achieved by tuning the polarization controller (PC) within the nonlinear polarization rotation (NPR) settings at fixed pump strength. Our present work first establishes a general, deterministic route to induce soliton breathing in normal dispersion mode-locked fiber lasers. Moreover, we directly reveal both the spectral and temporal dynamics of breathing solitons using advanced measurement techniques and

[1]State Key Laboratory of Precision Spectroscopy, East China Normal University, Shanghai 200062, China. [2]Aston Institute of Photonic Technologies, School of Engineering and Applied Science, Aston University, Birmingham B4 7ET, UK.
*Corresponding author. Email: hpzeng@phy.ecnu.edu.cn

dispersion engineering, which enables the generation of breathers with durations close to the resolution of state-of-the-art oscilloscopes.

RESULTS

Experimental setups

The output of a mode-locked fiber laser depends strongly on the net dispersion of the laser cavity. When operating in the anomalous dispersion regime, a laser emits pulses with shapes close to the hyperbolic secant profile of a conventional soliton. When the dispersion is close to zero, stretched pulses with Gaussian profiles are generated. Mode-locked fiber lasers working in the normal dispersion regime can output pulses with high energies as a result of a pulse-shaping process based on spectral filtering of a highly chirped pulse (*29*). These lasers are fundamental building blocks of various photonic systems, such as high-power pulse amplification systems, frequency combs, and others. The laser used in our experiment operates in the telecommunication optical band where the use of a dispersion compensating fiber (DCF) allows the laser to work in the normal dispersion regime. The laser setup is sketched in Fig. 1A. The cavity incorporates three types of fibers: a short length (1.4 m) of erbium-doped fiber (EDF) providing gain, DCF used for dispersion compensation, and standard single-mode fiber (SMF) from the pigtails of the optical components used. The group velocity dispersion (GVD) values of these fibers are 65, 62.5, and −22.8 ps^2/km, respectively. During the experiment, the length of the EDF was fixed, and dispersion management in the cavity was accomplished through variation of the relative length of DCF and SMF. The EDF is pumped through a 980/1550 wavelength division multiplexer by a 976-nm laser diode. The mode-locking mechanism is NPR, facilitated through the inclusion of a combination of two PCs and an in-fiber polarization-dependent isolator. As shown in Fig. 1B, the output of the laser is split into two paths by an optical coupler. One path (undispersed) is used to record the evolution of the instantaneous intensity pattern $I(t)$. The signal from the other port is fed into a long (~11 km in our experiment) normally dispersive fiber to temporally stretch the pulses and thus acquire TS-DFT–based spectral measurements (*24*, *25*). The signals from the two paths are detected by two identical high-speed photodetectors (PD1 and PD2) with a bandwidth of 50 GHz and captured by a real-time oscilloscope with a sampling rate of 80 gigasamples per second and a bandwidth of 33 GHz (Keysight DSAV334A), which ensures a resolution of ~0.025 nm for the TS-DFT measurements. Note that by measuring the temporal delay between the two photodetectors (53.651 μs), we were able to take simultaneous measurements of the spectral and temporal intensities of the output pulses.

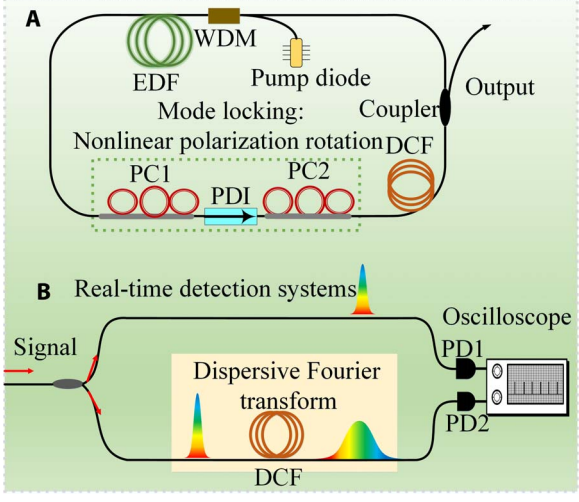

Fig. 1. Experimental setups. (**A**) Schematic of the breathing DS fiber laser. WDM, wavelength division multiplexer; PDI, polarization-dependent isolator. (**B**) Schematic of the real-time detection system, realizing synchronous measurements of the temporal intensity and the spectra of breathers. PD, photodetector.

The principle of the TS-DFT technique consists of stretching an optical pulse in a dispersive medium that cumulates a GVD large enough to map the optical spectrum into the temporal domain, which is a conceptual analog to the far-field limit in paraxial diffraction (*24*). Benefiting from the fast response time of a photodetector, DFT can record spectra at a scan rate remarkably higher than those of conventional space-domain spectrometers. This enables the measurement of round-trip resolved spectra, which has recently helped reveal various fast dynamics in lasers (*15*, *16*, *25*, *26*, *30*–*32*). The methodology of spatiotemporal dynamics relies on measuring time traces of one-dimensional intensity in real time, $I(t)$, and then, by using a wide-band real-time digital storage oscilloscope, constructs from these traces the spatiotemporal intensity dynamics $I(t,z)$ (*33*). The latter reveals both the dynamics over the fast time t and the slow evolution propagation coordinate z, which is measured, in our case, as a number of cavity round trips. The combination of real-time TS-DFT spectral measurements with the real-time spatiotemporal methodology in our experiment provides a time-aligned spectro- and spatiotemporal characterization of the DS breathing process.

Experimental observation of breathing solitons

Our laser is a typical normal dispersion fiber laser that can emit stationary DSs with rectangular spectra when it is mode-locked through NPR. The question is how to trigger breathing DSs in this laser. We have found that there exist two mechanisms through which breathing DSs can be excited in the laser. A first, fully controllable way of accessing breathers relies on decreasing the pump strength starting from stationary DS mode locking. Alternatively, breathers can also be induced through rotation of the PCs within the NPR settings starting from a continuous-wave regime in which the pump power is below the threshold for stationary mode locking. These two procedures for accessing the breathing laser state were verified across a large range of net cavity dispersion values from 0.002 to 0.14 ps^2, thereby establishing that a new operation regime of the laser, the breather mode-locking regime, exists under the threshold of standard mode locking.

Figure 2 presents the experimental results obtained for a net cavity dispersion of 0.14 ps^2. This large dispersion leads to the generation of broad pulses that can be directly detected by a photodetector. Above this dispersion value, no stationary mode locking existed, and only noise-like pulses were emitted from the laser. Figure 2 (A and B) shows the respective spectral and temporal evolutions of a breathing DS over cavity round trips, as recorded by TS-DFT and spatiotemporal intensity measurements. The validation of our implementation of the TS-DFT technique is presented in the Supplementary Materials. The pulse spectrum compresses and stretches periodically with a period of approximately 170 cavity round trips (Fig. 2A). Note that such a fast evolution is beyond the speed of a traditional optical spectrum analyzer. Although the pulse duration is close to the resolution of the detection system (30 ps), breathing dynamics in the temporal domain are clearly revealed in Fig. 2B. The evolution of the pulse temporal profile over cavity round trips is periodic, and the peak intensity varies within each

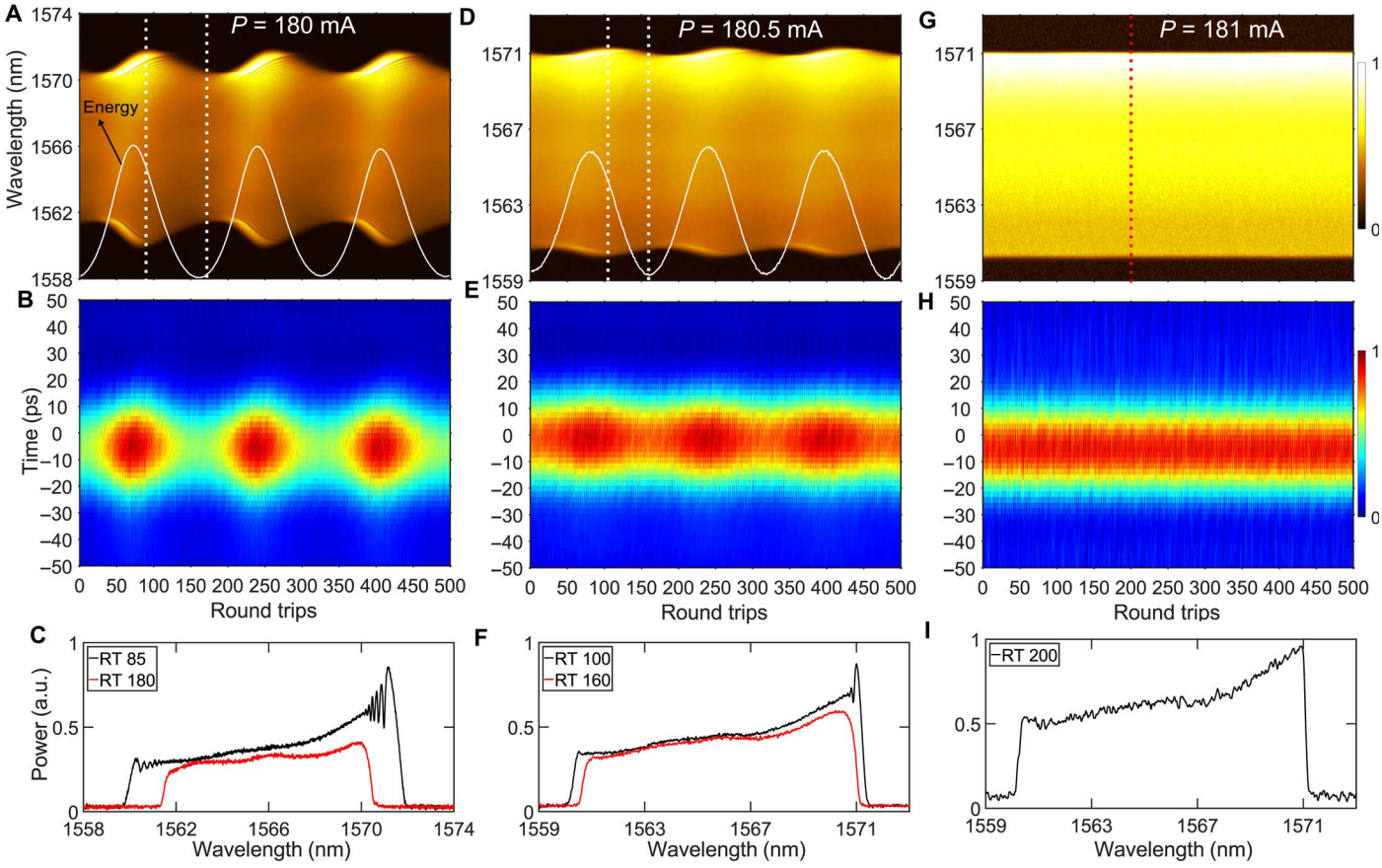

Fig. 2. Experimental observation of breathing DSs in a normal dispersion mode-locked fiber laser. (**A** to **C**) Dynamics of a breather at a pump current of 180 mA. (A) TS-DFT recording of single-shot spectra over 500 consecutive round trips. (B) Temporal evolution of the intensity relative to the average round-trip time over 500 consecutive round trips. (C) Single-shot spectra at the round-trip (RT) numbers of maximal and minimal spectrum extents within a period. (**D** to **F**) Dynamics of a breather at a pump current of 180.5 mA. (D) TS-DFT recording of single-shot spectra over consecutive round trips. (E) Temporal evolution of the intensity relative to the average round-trip time over consecutive round trips. (F) Single-shot spectra at the round-trip numbers of maximal and minimal spectrum extents within a period. (**G** to **I**) Stationary DS at a pump current of 181 mA. (G) TS-DFT recording of single-shot spectra over consecutive round trips. (H) Temporal evolution of the intensity relative to the average round-trip time over consecutive round trips. (I) Exemplary single-shot spectrum. The net cavity dispersion is 0.14 ps^2. a.u., arbitrary units.

period, with the highest (lowest) peak intensity naturally occurring in the vicinity of the position where the spectrum reaches the largest (narrowest) width. We have also calculated the energy of the pulse by integrating its power spectral density over the whole wavelength band. The evolution of the energy over cavity round trips is shown in Fig. 2A (white curve). The highest energy within each period exceeds the minimal one by nearly two times. Figure 2C shows the pulse spectra at the round-trip numbers of maximal and minimal spectrum extents within a period. One can see the development of fringes at the edges of the spectrum (black curve), which relate to shock wave dynamics occurring in normal dispersion mode-locked fiber lasers (*34*).

Starting from this breather generation regime, increasing the pump power resulted in an increasingly smaller breathing ratio (defined as the ratio of the largest to the narrowest spectrum width within a period) until the breathing ratio reached the value of one, meaning that a stationary DS had formed. This process is illustrated in Fig. 2 (A, D, and G), in which the pump current is increased gradually. While the breathing ratio is 1.35 in Fig. 2A, it is 1.05 in Fig. 2B. Such a relationship between pump power and breathing ratio was also verified in laser cavities with varied dispersion. Two examples are provided in the Supplementary Materials, corresponding to net cavity dispersions of 0.03 and 0.1 ps^2. We ascribe this relationship to the saturation of the energy of the pulse with the broadest spectrum. As a consequence, an increase in pump power only transfers energy to the weak pulses, hence entailing a reduced breathing ratio. The process is reversible: By decreasing the pump power, the stationary DS returned to the breathing state. We would like to note that the breather mode-locking regime observed in our experiment is rather different from Q-switched mode locking (QML) related to undamped relaxation oscillations. The former features pulses with a large spectral width (~20 nm), while the latter is distinguished by typical pulse spectral widths of a few nanometers. Furthermore, the modulation frequency of the breathers here is around 1 MHz, while QML is characterized by modulation frequencies in the kilohertz range in EDF lasers. Last, the results of numerical simulations of the laser dynamics are in agreement with our experimental observations, while the laser model used does not include Q-switching instabilities (see the "Simulations" section).

Breathing soliton molecules

In specific parameter ranges, the coherent interactions between several solitons coexisting in a laser cavity may lead to the self-assembly of stable multisoliton bound states (*35*), which are frequently termed soliton

molecules in virtue of their analogy with matter molecules (*36*). Recently, real-time access to multipulse interactions in laser oscillators has made it possible to track the formation of soliton molecules and uncover different types of rapid internal motions (*15*–*17*). It is inherently interesting to know whether breathers can also cluster together into bound states (breathing soliton molecules). Notably, in addition to the single breathing DSs described above, we also observed breathing soliton pair molecules in our experiment. They were found when the net dispersion of the cavity was decreased to 0.002 ps^2. A laser with smaller dispersion is prone to generate multiple pulses because the higher peak power of the pulses (corresponding to a short pulse duration) is saturated by the peak-power clamping effect in the NPR mode-locked laser. Figure 3A shows the shot-to-shot spectral evolution of a breather molecule over cavity round trips as measured by the TS-DFT. The spectrum of the breather pair features the typical interference pattern that is present in the spectrum of a soliton molecule (*15*). The single-shot spectra of the largest and narrowest widths within a period are depicted in Fig. 3B (the intensity is offset for better visibility). Although the spectral width experiences large periodic variations, the separation between the peaks of spectral intensity remains fixed at 0.18 nm over consecutive round trips. Constant spectral peak spacing implies a constant pulse separation in the time domain. The corresponding spatiotemporal intensity dynamics shown in Fig. 3C reveal that the intramolecular temporal separation has a constant value of 45 ps, which is in excellent agreement with the spectral peak separation value. Figure 3D shows the temporal intensity profiles at the round-trip numbers of maximal and minimal spectrum extents. We have also investigated the temporal dynamics of the breather molecule using field autocorrelation analysis (*15*), which showed good agreement with Fig. 3C (see the Supplementary Materials for details).

Besides breather pair molecules with a close pulse separation, we also observed bound double breathing solitons widely separated by 34 ns when the net cavity dispersion was increased relative to the molecule state. Since the pulse spacing was so large, the TS-DFT could resolve the spectrum of each individual pulse. The measured TS-DFT data are shown in Fig. 4A. The breathing period is approximately 120 cavity round trips, close to the period of the breather molecule described above. Note that the central wavelengths of the two breathers are equal; the pulse separation would otherwise evolve over time because of dispersion. Figure 4B presents the corresponding temporal information obtained from the photodetector. The time axis is broken in Fig. 4B to clearly visualize the breathing dynamics. The mechanism responsible for binding of these largely spaced pulses can be deemed to be a pulse interaction mediated by acoustic waves (*37*).

Both the breather pair molecules and bound double breathers described above feature a synchronous (in-phase) evolution of the elementary soliton temporal intensities with the cavity round trips. On the other hand, we have also found another type of bound double breathing

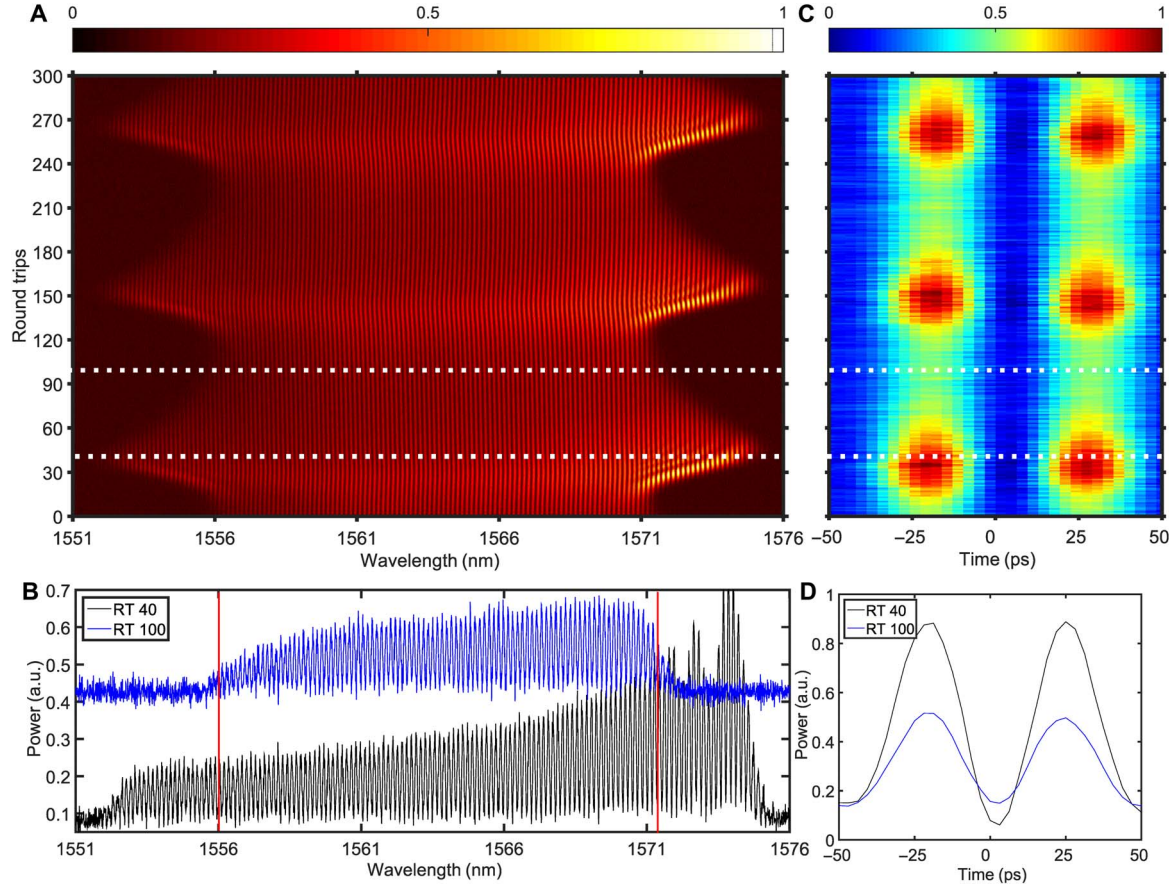

Fig. 3. Dynamics of a breathing soliton pair molecule. (**A**) TS-DFT recording of the shot-to-shot spectral evolution, showing a modulated spectrum. (**B**) Single-shot spectra at the round-trip numbers of maximal and minimal spectrum extents within a period. (**C**) Temporal intensity evolution relative to the average round-trip time; (**D**) Temporal intensity profiles at the round-trip numbers of maximal and minimal spectrum extents within a period.

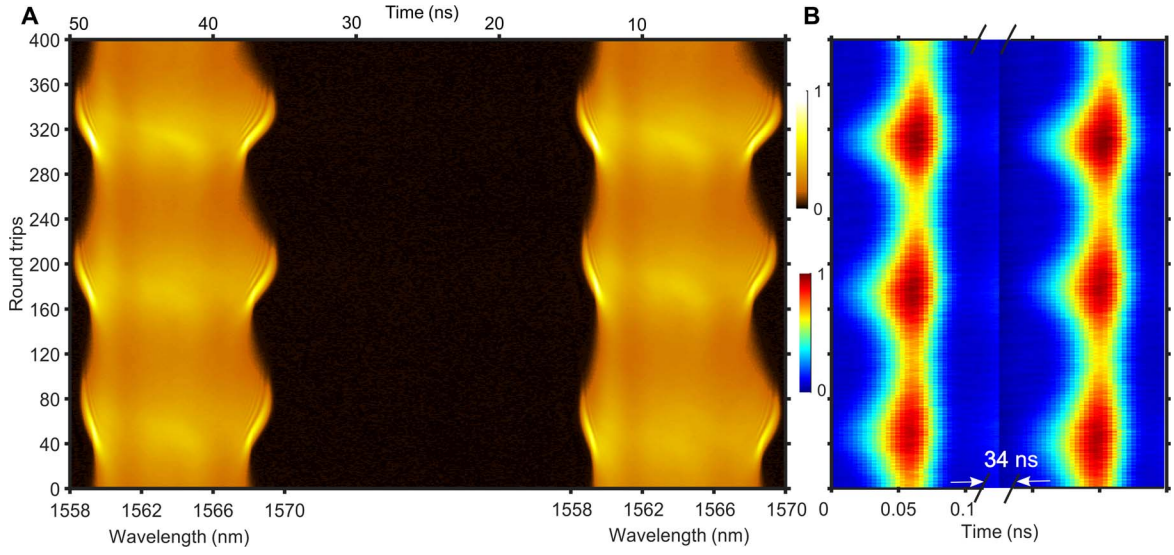

Fig. 4. Dynamics of a bound breathing soliton pair with a large pulse separation (~34 ns). (**A**) TS-DFT recording of the shot-to-shot spectral evolution. Owing to the large pulse separation, the spectrum of each individual pulse can be resolved by the TS-DFT. (**B**) Temporal intensity evolution relative to the average round-trip time. Note that the time axis is broken to highlight the breathing dynamics.

soliton in the laser, an asynchronous breather pair, in which the pulsations of the individual intensities are asynchronous (see the Supplementary Materials).

SIMULATIONS

To ascertain whether the observed laser behaviors are general, we carried out numerical simulations of the laser based on the master equation approach (see Materials and Methods), which is one of the main techniques used in the theory of passively mode-locked lasers (*20*, *21*). This approach was first suggested by Haus (*38*) and later developed into a cubic-quintic Ginzburg-Landau equation (CQGLE) as the equation of minimal complexity that admits stable soliton solutions, thus allowing us to describe pulse generation phenomena by optical oscillators. The experimental results indicate that the gain coefficient is critical in triggering the transitions between breathing and stationary soliton states. In the CQGLE, the parameter θ relates to the gain and loss of the system (see Materials and Methods). Figure 5 shows typical examples of the solutions to the CQGLE that we have found numerically for θ = −0.1 and θ = 0.05 and the set of other parameters given in the caption. Figure 5 (A and B) (θ = −0.1) shows periodic breathing dynamics of a single pulse. The evolutions of the peak power of the soliton at its center, τ = 0, and the pulse energy $Q(\zeta) = \int |\psi(\zeta, \tau)|^2 d\tau$ with the propagation coordinate ζ are plotted in fig. S6. The spectrum widens at the positions of the spikes of temporal intensity creating subsequently discrete sidebands symmetrically located at each side. The latter decays quickly before the next spike is generated. For a net cavity dispersion of 0.14 ps^2 and taking the unit of the dimensionless variable τ to be 2 ps, the period of oscillation in our simulation is approximately 170 cavity round trips, in accordance with the experiment. Increasing the parameter θ to 0.05, we observed that the pulse solution stabilizes to a stationary state after an initial transient stage (Fig. 5, C and D). While the pulse solution shown in Fig. 5 (A and B) and fig. S6 exhibits the qualitative features of the experimentally observed breathing solitons, it resembles the strongly pulsating solitons demonstrated theoretically in (*23*). We

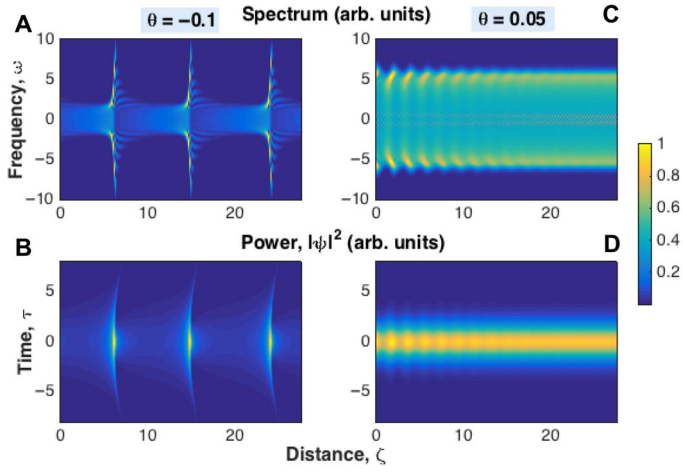

Fig. 5. Simulation of the transition between breathing DSs and stable DSs. Evolutions of the spectrum and temporal intensity of the solutions of the CQGLE found for θ = −0.1 (subplots **A** and **B**) and θ = 0.05 (subplots **C** and **D**). The other CQGLE parameters are (*D*, η, ε, β, μ) = (−1, 0.21, 0.4, 0.125, 0.008).

would like to point out, however, that theoretical modeling is used here to qualitatively account for the observed pulse dynamics rather than to provide an accurate quantitative comparison with the experiment. In this light, comparison of Figs. 2 and 5 makes a strong case that the formation of breathers is ubiquitous in normal dispersion mode-locked fiber lasers when they are operated below the pump threshold for stationary mode locking. Figure 6 shows an example of a breathing soliton pair molecule that we have found by solving the CQGLE numerically. Again, this simulation should be regarded in the same light as discussed above, that is, as a qualitative and descriptive picture of breather molecule formation in the laser rather than a quantitative account for the observed molecule dynamics.

Our CQGLE simulations revealed that nonlinear dissipative terms are crucial for the generation of breathers. No breathers were found when the quintic gain/loss coefficient (μ) was set to zero. We

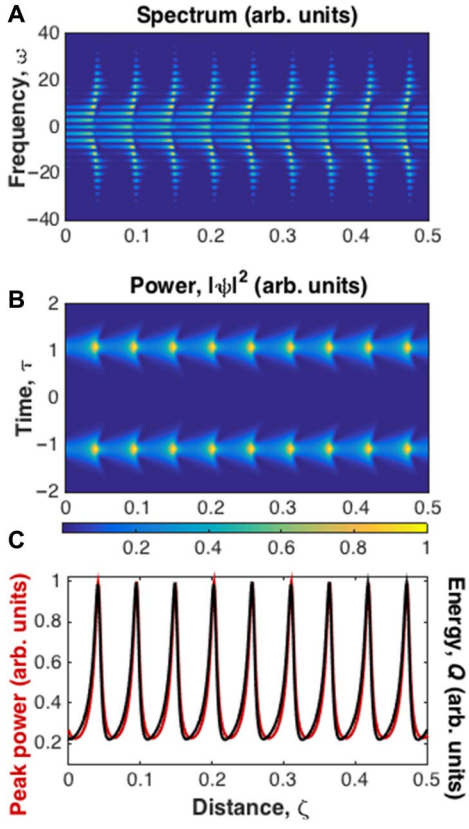

Fig. 6. Simulation of breathing soliton molecules. (**A** and **B**) Evolutions of the spectrum and temporal intensity of a typical breather pair molecule solution of the CQGLE. (**C**) Evolutions of the pulse peak power and energy for the same simulation.

also performed numerical simulations of a lumped model of the laser in which pulse propagation in the fiber sections is described by the generalized standard nonlinear Schrödinger equation (NLSE). However, we could not find breather solutions in this case. This may be ascribed to the fact that the NLSE only accounts for the effects of linear gain/loss and gain bandwidth. The effect of quintic gain/loss relates to the mode-locking mechanism (*39*). While such an effect plays a pivotal role in stabilizing mode locking in the anomalous dispersion regime, our work shows that it is central to the generation of breathers at normal dispersion.

DISCUSSION

We have experimentally demonstrated the formation of breathing DSs in a normal dispersion passively mode-locked fiber laser. This pulse generation regime is induced in the laser cavity by operating the laser under the pump threshold for stationary DS mode locking. This is in sharp contrast to the breather operational regime of anomalous dispersion mode-locked fiber lasers: It has been shown numerically that breathers may be induced in a laser cavity with anomalous dispersion by increasing the pump level from the threshold for stationary soliton mode locking (*40*). Furthermore, solely changing the pump strength to access the breather regime from continuous-wave mode locking in our experiment clearly indicates that the breathers result from a Hopf bifurcation. The universal nature of the breather formation revealed here is indicated by our observation in a varying-length cavity and further confirmed by numerical simulations of the laser model described by the complex CQGLE. Breathing soliton pair molecules have also been observed in experiments with mode-locked fiber lasers.

Fiber lasers are well known for their versatile design such as ring, linear, figure 8, figure 9, and theta cavities, as well as their compatibility with a rich variety of mode-locking mechanisms, including saturable absorbers based on various materials and multimode fibers. It is therefore of significant interest to explore the excitation of breathers in fiber laser cavities with different characteristics and operating conditions.

Our results demonstrate that breathers are intrinsically present in the dynamics of normal dispersion mode-locked fiber lasers. These lasers constitute the building blocks of high-power pulse amplification systems owing to their superior energy and peak power performances relative to lasers working in the anomalous dispersion regime. However, the occurrence of soliton breathing could undermine the stability of these systems, and our work indicates an unambiguous way to avoid such a phenomenon. Our findings not only carry importance from an application perspective but also contribute more broadly to the fundamental understanding of DS physics. Our observations further demonstrate that mode-locked fiber lasers are an ideal test bed for the study of complex nonlinear wave dynamics relevant to a large variety of physical systems. Potentially, similar soliton breathing behavior could also exist in ultrafast Ti:sapphire and semiconductor lasers. More generally, the complex CQGLE is the most common mathematical implementation of a dissipative system, describing many different nonlinear effects in physics, such as nonlinear waves, superconductivity, superfluidity, Bose-Einstein condensates, liquid crystals, plasmas, and numerous other phenomena. Therefore, it is reasonable to assume that the breathing DS dynamics found in this work are not limited to optical systems and will also be discovered in various other physical systems.

MATERIALS AND METHODS

Numerical modeling

For our passively mode-locked laser model, we used the complex CQGLE, which, in its standard form, reads as (*1*)

$$i\Psi_\xi + \frac{D}{2}\Psi_{\tau\tau} + |\Psi|^2\Psi + \eta|\Psi|^4\Psi = i\theta\Psi + i\varepsilon|\Psi|^2\Psi + i\beta\Psi_{\tau\tau} + i\mu|\Psi|^4\Psi \quad (1)$$

where τ is the normalized time in a frame of reference moving with the group velocity, ψ is the complex envelope of the optical field, and ζ is the propagation distance along the unfolded cavity. The units of the dimensionless time and space variables are a characteristic temporal value of the pulse T_0 and the dispersion length $L_D = T_0^2/|\bar{\beta}_2|$, respectively, where $\bar{\beta}_2$ is the path-averaged dispersion of the cavity. On the left-hand side, $D = -\mathrm{sgn}(\bar{\beta}_2)$, and η is the quintic refractive index coefficient. The dissipative terms are written on the right-hand side of Eq. 1, where θ denotes the net linear gain/loss, β is the gain bandwidth coefficient, and ε and μ are the cubic and quintic gain/loss coefficients, respectively. The continuous laser model described by Eq. 1 has an analog in the corresponding lumped model, and the parameter θ is directly related to the small-signal gain of the active fiber; thus, it plays a similar role to the pump power in the experiment.

SUPPLEMENTARY MATERIALS

Supplementary material for this article is available at http://advances.sciencemag.org/cgi/content/full/5/11/eaax1110/DC1

Fig. S1. Validation of the TS-DFT implementation.

Fig. S2. Breathing soliton dynamics observed when the net dispersion of the laser cavity is 0.03 ps^2.

Fig. S3. Breathing soliton dynamics observed when the net dispersion of the laser cavity is 0.1 ps^2.

Fig. S4. Dynamics of a breathing soliton pair molecule.

Fig. S5. Temporal dynamics of asynchronous bound breathing soliton pair: The pulsations of the elementary soliton intensities over cavity round trips are not synchronous.

Fig. S6. Evolutions of the pulse peak power at its center $|\psi(\zeta, \tau = 0)|^2$ (red line) and the pulse energy $Q(\zeta)$ (black line) for the breather solution of the CQGLE shown in Fig. 5.

REFERENCES AND NOTES

1. P. Grelu, N. Akhmediev, Dissipative solitons for mode-locked lasers. *Nat. Photonics* **6**, 84–92 (2012).
2. N. Akhmediev, A. Ankiewicz, *Dissipative Solitons: From Optics To Biology And Medicine* (Springer, 2008).
3. F. Leo, L. Gelens, P. Emplit, M. Haelterman, S. Coen, Dynamics of one-dimensional Kerr cavity solitons. *Opt. Express* **21**, 9180–9191 (2013).
4. M. Yu, J. K. Jang, Y. Okawachi, A. G. Griffith, K. Luke, S. A. Miller, X. Ji, M. Lipson, A. L. Gaeta, Breather soliton dynamics in microresonators. *Nat. Commun.* **8**, 14569 (2017).
5. E. Lucas, M. Karpov, H. Guo, M. L. Gorodetsky, T. J. Kippenberg, Breathing dissipative solitons in optical microresonators. *Nat. Commun.* **8**, 736 (2017).
6. C. Bao, J. A. Jaramillo-Villegas, Y. Xuan, D. E. Leaird, M. Qi, A. M. Weiner, Observation of Fermi-Pasta-Ulam recurrence induced by breather solitons in an optical microresonator. *Phys. Rev. Lett.* **117**, 163901 (2016).
7. A. Mussot, C. Naveau, M. Conforti, A. Kudlinski, F. Copie, P. Szriftgiser, S. Trillo, Fibre multi-wave mixing combs reveal the broken symmetry of Fermi–Pasta–Ulam recurrence. *Nat. Photonics* **12**, 303–308 (2018).
8. P. Suret, R. El Koussaifi, A. Tikan, C. Evain, S. Randoux, C. Szwaj, S. Bielawski, Single-shot observation of optical rogue waves in integrable turbulence using time microscopy. *Nat. Commun.* **7**, 13136 (2016).
9. J. M. Dudley, F. Dias, M. Erkintalo, G. Genty, Instabilities, breathers and rogue waves in optics. *Nat. Photonics* **8**, 755–764 (2014).
10. J. Soto-Crespo, N. Devine, N. Akhmediev, Integrable turbulence and rogue waves: Breathers or solitons? *Phys. Rev. Lett.* **116**, 103901 (2016).
11. M. Närhi, B. Wetzel, C. Billet, S. Toenger, T. Sylvestre, J.-M. Merolla, R. Morandotti, F. Dias, G. Genty, J. M. Dudley, Real-time measurements of spontaneous breathers and rogue wave events in optical fibre modulation instability. *Nat. Commun.* **7**, 13675 (2016).
12. P. Liao, K. Zou, C. Bao, A. Kordts, M. Karpov, M. H. P. Pfeiffer, L. Zhang, Y. Cao, A. Almaiman, F. Alishashi, A. Mohajerin-Ariaei, A. Fallahpour, M. Tur, T. J. Kippenberg, A. E. Willner, "Chip-scale dual-comb source using a breathing soliton with an increased resolution," paper presented at the Conference on Lasers and Electro-Optics, San Jose, CA, 13 to 18 May 2018.
13. D. Solli, C. Ropers, P. Koonath, B. Jalali, Optical rogue waves. *Nature* **450**, 1054–1057 (2007).
14. C. Lecaplain, P. Grelu, J. Soto-Crespo, N. Akhmediev, Dissipative rogue waves generated by chaotic pulse bunching in a mode-locked laser. *Phys. Rev. Lett.* **108**, 233901 (2012).
15. G. Herink, F. Kurtz, B. Jalali, D. R. Solli, C. Ropers, Real-time spectral interferometry probes the internal dynamics of femtosecond soliton molecules. *Science* **356**, 50–54 (2017).
16. K. Krupa, K. Nithyanandan, U. Andral, P. Tchofo-Dinda, P. Grelu, Real-time observation of internal motion within ultrafast dissipative optical soliton molecules. *Phys. Rev. Lett.* **118**, 243901 (2017).
17. J. Peng, H. Zeng, Build-up of dissipative optical soliton molecules via diverse soliton interactions. *Laser Photon. Rev.* **12**, 1800009 (2018).
18. Z. Wang, K. Nithyanandan, A. Coillet, P. Tchofo-Dinda, P. Grelu, Optical soliton molecular complexes in a passively mode-locked fibre laser. *Nat. Commun.* **10**, 830 (2019).
19. Z. Wang, Z. Wang, Y. Liu, R. He, J. Zhao, G. Wang, G. Yang, Self-organized compound pattern and pulsation of dissipative solitons in a passively mode-locked fiber laser. *Opt. Lett.* **43**, 478–481 (2018).
20. J. M. Soto-Crespo, N. Akhmediev, A. Ankiewicz, Pulsating, creeping, and erupting solitons in dissipative systems. *Phys. Rev. Lett.* **85**, 2937–2940 (2000).
21. S. T. Cundiff, J. M. Soto-Crespo, N. Akhmediev, Experimental evidence for soliton explosions. *Phys. Rev. Lett.* **88**, 073903 (2002).
22. A. F. Runge, N. G. Broderick, M. Erkintalo, Observation of soliton explosions in a passively mode-locked fiber laser. *Optica* **2**, 36–39 (2015).
23. W. Chang, J. M. Soto-Crespo, P. Vouzas, N. Akhmediev, Extreme soliton pulsations in dissipative systems. *Phys. Rev. E Stat. Nonlin. Soft Matter Phys.* **92**, 022926 (2015).
24. K. Goda, B. Jalali, Dispersive Fourier transformation for fast continuous single-shot measurements. *Nat. Photonics* **7**, 102–112 (2013).
25. A. F. Runge, C. Aguergaray, N. G. Broderick, M. Erkintalo, Coherence and shot-to-shot spectral fluctuations in noise-like ultrafast fiber lasers. *Opt. Lett.* **38**, 4327–4330 (2013).
26. A. Mahjoubfar, D. V. Churkin, S. Barland, N. Broderick, S. K. Turitsyn, B. Jalali, Time stretch and its applications. *Nat. Photonics* **11**, 341–351 (2017).
27. G. Xu, A. Gelash, A. Chabchoub, V. Zakharov, B. Kibler, Breather wave molecules. *Phys. Rev. Lett.* **122**, 084101 (2019).
28. Y. Du, Z. Xu, X. Shu, Spatio-spectral dynamics of the pulsating dissipative solitons in a normal-dispersion fiber laser. *Opt. Lett.* **43**, 3602–3605 (2018).
29. F. W. Wise, A. Chong, W. H. Renninger, High-energy femtosecond fiber lasers based on pulse propagation at normal dispersion. *Laser Photon. Rev.* **2**, 58–73 (2008).
30. G. Herink, B. Jalali, C. Ropers, D. R. Solli, Resolving the build-up of femtosecond mode-locking with single-shot spectroscopy at 90 MHz frame rate. *Nat. Photonics* **10**, 321–326 (2016).
31. K. Krupa, K. Nithyanandan, P. Grelu, Vector dynamics of incoherent dissipative optical solitons. *Optica* **4**, 1239–1244 (2017).
32. P. Ryczkowski, M. Närhi, C. Billet, J.-M. Merolla, G. Genty, J. M. Dudley, Real-time full-field characterization of transient dissipative soliton dynamics in a mode-locked laser. *Nat. Photonics* **12**, 221–227 (2018).
33. D. Churkin, S. Sugavanam, N. Tarasov, S. Khorev, S. V. Smirnov, S. M. Kobtsev, S. K. Turitsyn, Stochasticity, periodicity and localized light structures in partially mode-locked fibre lasers. *Nat. Commun.* **6**, 7004 (2015).
34. C. Lecaplain, J. M. Soto-Crespo, P. Grelu, C. Conti, Dissipative shock waves in all-normal-dispersion mode-locked fiber lasers. *Opt. Lett.* **39**, 263–266 (2014).
35. B. A. Malomed, Bound solitons in the nonlinear Schrödinger-Ginzburg-Landau equation. *Phys. Rev. A* **44**, 6954–6957 (1991).
36. M. Stratmann, T. Pagel, F. Mitschke, Experimental observation of temporal soliton molecules. *Phys. Rev. Lett.* **95**, 143902 (2005).
37. J. K. Jang, M. Erkintalo, S. G. Murdoch, S. Coen, Ultraweak long-range interactions of solitons observed over astronomical distances. *Nat. Photonics* **7**, 657–663 (2013).
38. H. A. Haus, Theory of mode locking with a fast saturable absorber. *J. Appl. Phys.* **46**, 3049–3058 (1975).
39. L. E. Nelson, D. J. Jones, K. Tamura, H. A. Haus, E. P. Ippen, Ultrashort-pulse fiber ring lasers. *Appl. Phys. B* **65**, 277–294 (1997).
40. B. G. Bale, K. Kieu, J. N. Kutz, F. Wise, Transition dynamics for multi-pulsing in mode-locked lasers. *Opt. Express* **17**, 23137–23146 (2009).

Acknowledgments

Funding: We acknowledge the support from the National Natural Science Fund of China (11434005, 11621404, 11561121003, 61775059, and 11704123), National Key Research and Development Program (2018YFB0407100), and Key Project of Shanghai Education Commission (2017-01-07-00-05-E00021). **Author contributions:** J.P. performed the experiments. S.B. carried out the numerical simulations with inputs from Z.Z. and J.P. H.Z., J.P., and S.B. analyzed the results. H.Z., J.P., and S.B. wrote the paper. H.Z. and S.B. supervised and guided the project. **Competing interests:** The authors declare that they have no competing interests. **Data and materials availability:** All data needed to evaluate the conclusions in the paper are present in the paper and/or the Supplementary Materials. Additional data related to this paper may be requested from H.Z. (hpzeng@phy.ecnu.edu.cn).

Submitted 22 February 2019
Accepted 17 September 2019
Published 1 November 2019
10.1126/sciadv.aax1110

Citation: J. Peng, S. Boscolo, Z. Zhao, H. Zeng, Breathing dissipative solitons in mode-locked fiber lasers. *Sci. Adv.* **5**, eaax1110 (2019).

Science Advances

Breathing dissipative solitons in mode-locked fiber lasers

Junsong Peng, Sonia Boscolo, Zihan Zhao and Heping Zeng

Sci Adv **5** (11), eaax1110.
DOI: 10.1126/sciadv.aax1110